

Sea-level probability for the last deglaciation: a statistical analysis of far-field records.

J.D. Stanford¹, R. Hemingway¹, E.J. Rohling¹, P.G. Challenor², M. Medina-Elizalde¹ and A. J. Lester³

¹School of Ocean and Earth Science, University of Southampton, National Oceanography Centre, Southampton SO14 3ZH, United Kingdom.

²National Oceanography Centre, Southampton, SO14 3ZH, United Kingdom.

³The Chamber of Shipping, 12 Carthusian Street, London, EC1M 6EZ.

Abstract

Pulses of ice-sheet meltwater into the world ocean during the last deglaciation are of great current interest, because these large-scale events offer important test-beds for numerical models of the responses of ocean circulation and climate to meltwater addition. The largest such event has become known as meltwater pulse (mwp) 1a, with estimates of about 20 m of sea-level rise in about 500 years. A second meltwater pulse (mwp-1b) has been inferred from some sea-level records, but its existence has become debated following the presentation of additional records. Even the use of the more ubiquitous mwp-1a in modelling studies has been compromised by debate about its exact age, based upon perceived discrepancies between far-field sea-level records. It is clear that an objective investigation is needed to determine to what level inferred similarities and/or discrepancies between the various deglacial sea-level records are statistically rigorous (or not). For that purpose, we present a Monte Carlo style statistical analysis to determine the highest-probability sea-level history from six key

far-field deglacial sea-level records, which fully accounts for realistic methodological and chronological uncertainties in all these records, and which is robust with respect to removal of individual component datasets. We find that sea-level rise started to accelerate into the deglaciation from around 17 ka BP. Within the deglacial rise, there were two distinct increases; one at around the timing of the Bølling warming (14.6 ka BP), and another, much broader, event that just post-dates the end of the Younger Dryas (11.3 ka BP). We interpret these as mwp-1a and mwp-1b, respectively. We find that mwp-1a occurred between 14.3 ka BP and 12.8 ka BP. Highest rates of sea-level rise occurred at ~13.8 ka, probably (67% confidence) within the range 100-130 cm/century, although values may have been as high as 260 cm/century (99% confidence limit). Mwp-1b is robustly expressed as a broad multi-millennial interval of enhanced rates of sea-level rise between 11.5 ka BP and 8.8 ka BP, with peak rates of rise of up to 250 cm/century (99 % confidence), but with a probable rate of 130 - 150 cm/century (67 % confidence) at around 9.5 ka BP. When considering the 67 % probability interval for the deglacial sea-level history, it is clear that both mwp1a and 1b were relatively subdued in comparison to the previously much higher rate estimates.

Key words: meltwater pulse, sea-level, deglaciation

1. Introduction

Since the Last Glacial Maximum (LGM), sea level has risen by around 120 m or so (e.g., Fairbanks, 1989; Bard et al., 1990a; b; 1996; Lambeck et al., 2002; Siddall et al., 2003; Peltier and Fairbanks, 2006). Proxy records used to constrain the sea-level

history since ~20 ka BP (thousands of years Before Present, where Present refers to AD1950) include datings on fossil coral terraces (Lighty et al., 1982; Fairbanks, 1989; Bard et al., 1990a; b; 1996; 2010; Chappell and Polach, 1991; Cutler et al., 2003; Fairbanks et al., 2005, Peltier and Fairbanks, 2006), and on plant fragments and calcareous marine organisms contained within marine sediment cores (Hanebuth et al., 2000; 2009; Yokoyama et al., 2000; 2001; Toscano and Macintyre, 2003 and references therein). However, the magnitudes of deglacial sea-level changes in each individual record are affected by isostatic adjustments, and therefore the information gained indicates the local (relative) sea-level change rather than the eustatic change (Figure 1) (e.g., Basset et al., 2005; Milne and Mitrovica, 2008). Additional to isostatic rebound uncertainties, our understanding of how the ocean-climate system has responded to deglacial freshwater forcings has been compromised because of depth and age uncertainties of sea-level indicators within individual proxy records.

For example, two key sea-level proxies (the Barbados U/Th-dated fossil coral and the Sunda Shelf radiocarbon-dated record of flooded coastline), appear to suggest different ages for meltwater pulse (mwp)-1a. Six recently added high-precision pre-mwp-1a U/Th datings in the Barbados record were found to comprehensively validate the original U/Th age of 14.2 ka BP for the onset of mwp-1a, although the new methods more precisely re-dated this onset to 14.082 ± 0.028 ka BP (1σ) (Fairbanks et al., 2005; Peltier and Fairbanks, 2006; Stanford et al., 2006). In contrast, the radiocarbon-dated record from the Sunda Shelf has been used to suggest that mwp-1a started 300-500 years earlier (Hanebuth et al., 2000). Although the difference is relatively small in view of systematic and random dating uncertainties, it has led to the development of two very different climate scenarios for mwp-1a, based on

comparison of the two dating scenarios with Greenland ice-core $\delta^{18}\text{O}$ (temperature) records.

The first climate scenario relies on the younger (U-series) datings of ~ 14 ka BP in the Barbados fossil coral record. These would imply that mwp-1a coincided in time with the Older Dryas cooling event that terminated the Bølling warm episode (Figure 2a, b) (Fairbanks, 1989; Bard et al., 1990a; b; 1996; Liu and Milliman, 2004; Fairbanks et al., 2005, Peltier and Fairbanks, 2006; Stanford et al., 2006; Liu et al., 2009). A reconstruction of North Atlantic Deep Water (NADW) flow intensity over Eirik Drift, offshore southern Greenland, indicates a coincident ~ 200 year weakening of the Atlantic Meridional Overturning Circulation (AMOC) (Stanford et al., 2006). However, it should be noted that mwp-1a in Barbados is represented by a break in the coral stratigraphy (Fairbanks, 1989; Bard et al., 1990a, b). Therefore, the first post-mwp-1a coral dated in Barbados may represent (provides the age of) the recolonisation, rather than the end of the melt water pulse.

The second climate scenario relies on the older and less precise (radiocarbon) datings of 14.6 to 14.3 ka BP for mwp-1a from the Sunda Shelf (Figure 2c; Hanebuth et al., 2000). These would imply that mwp-1a coincided with the sharp Bølling warming (Figure 2a), when Greenland temperatures rose from glacial to near present-day values in only a decade or two (Severinghaus and Brook, 1999; Rasmussen et al., 2006). The AMOC underwent a major abrupt intensification at that time (McManus et al., 2004; Stanford et al., 2006). By comparing the magnitude of sea-level change for mwp-1a from Barbados and the Sunda Shelf to sea-level 'fingerprints' inferred from an Earth model of glacial isostatic adjustment, Clark et al. (2002) suggested that a

large component of mwp-1a originated from Antarctica. These findings were recently confirmed by a re-analysis of datings of glacial retreat evidence (Clark et al., 2009). An ocean circulation model suggested that if this large meltwater event had been sourced from Antarctica, at the timing suggested by the Sunda Shelf record, it could have caused the sharp AMOC resumption in the North Atlantic, and the attendant Bølling warming (Weaver et al., 2003).

More recently, a new continuous fossil coral record from Tahiti was used to test the existence of a second meltwater pulse, mwp-1b (Bard et al., 2010), which was originally identified in the Barbados fossil coral record between 11.5 - 11.1 ka BP (Fairbanks, 1989; Bard et al., 1990a,b) but was also associated with a break in the fossil coral stratigraphy. The latest record from Tahiti shows a nearly constant rate of sea-level rise during the post-Younger Dryas period, which seriously questions the initial interpretation of mwp-1b in Barbados (Bard et al., 2010). It is evident that for these deglacial meltwater pulses, a comprehensive statistical overview is needed of all available quality sea-level data, with their individual uncertainties.

Here we present a novel method for assessing the uncertainties in the compiled far-field sea-level reconstructions for the last deglaciation. It has been suggested by Earth models that the isostatic sea-level change at far-field sites would have been minimal during the deglaciation (e.g., Milne and Mitrovica, 2008) and hence, we use datasets from these (low latitude) regions. Using the combined data (and their given uncertainties) from six key sea-level reconstructions (Table 1), we use a Monte Carlo style method to establish the 99 % confidence margins of the sea-level history throughout the last deglaciation. We then evaluate which data fall outside the

reconstructed 99 % confidence interval for the onset of mwp-1a, and we investigate why this may be the case, in order to reconcile the (up until now) contentious sea-level records.

2. Methods

A first key step to our assessment is a recalibration of the originally reported radiocarbon convention ages from Sunda Shelf (Hanebuth et al., 2000; 2009), Bonaparte Gulf (Yokoyama et al., 2000; 2001), Huon Peninsula (Chappell and Polach, 1991) and Florida Keys and Caribbean Sea region (Toscano and Macintyre, 2003 and reference therein), and also for non U/Th dated samples from Tahiti (Bard et al., 1996). We do this using the INTCAL09/MARINE09 (Calib6.01) calibration curve (Reimer et al., 2009). Note that for mangrove wood, no reservoir correction is required because the carbon is acquired from atmospheric CO₂ (Reimer et al., 2004; 2009). In the absence of detailed reconstructions for every site, we assume that ΔR (change in reservoir age) equals zero for marine datings.

We use the Monte Carlo method to produce 99, 95 and 67 % probability envelopes for the combined sea-level reconstructions obtained from Sunda Shelf (Hanebuth et al., 2000; 2009), Bonaparte Gulf (Yokoyama et al., 2000; 2001), Houn Peninsula (Chappell and Polach, 1991; Cutler et al., 2003), Florida Keys and Caribbean Sea region (Toscano and Macintyre, 2003 and reference therein), Tahiti (Bard et al., 1996; 2010) and Barbados (Fairbanks, 1989; Bard et al., 1990a, b; Fairbanks et al., 2005; Peltier and Fairbanks, 2006), and each data point was perturbed according to their associated sea-level and age uncertainties (supplementary material 1). We compare

the analysis of the full dataset with analyses of partial datasets, made by “leaving one site out”, to establish that the overall results are robust and not disproportionately dependent on any of the component datasets. Note that we use the data after tectonic correction, but not isostatic correction, as we mainly use data from far-field sites (Figure 1, Table 1). Although the Toscano and Macintyre (2003) sea-level data compilation (crosses in Figure 1a) may not, in the strictest sense, be considered as ‘far-field’, these data constrain the last 8 kyrs only (Figure 1b) and therefore do not affect our main conclusions.

For uncertainties to the ages in all datasets, we assume a normal distribution, even though this is a slight simplification in the case of Accelerator Mass Spectrometric (AMS)¹⁴C ages. For all fossil coral depths, we assume a lognormal depth uncertainty to account for an up to 6 m habitat range for the species *Acropora palmata* (Lighty et al., 1982; Toscano and Macintyre, 2003). Note that we later include a sensitivity test in which this depth range is increased. We ascribe a probability distribution where water depths cannot be less than 0 on the basis that corals cannot live above the water level. For all other reconstructions which are based upon flooded shelf data (Hanebuth et al., 2000; 2009; Yokoyama 2000; 2001; Toscano and Macintyre and references therein), we use a Normal distribution for the given tidal ranges. For an overview of the data used, see Table 1.

The age and depth uncertainties for each data point were randomly perturbed according to their probability distributions and a smoothing spline (Green and Silverman, 1994) was fitted to the resulting ‘data’ using the `smooth.spline` function in the R language (R Development Core Team; 2010). The degrees of freedom for the

smoothing spline were obtained through (automated) generalised cross validation (Green and Silverman, 1994). In essence, generalised cross validation calculates the number of degrees of freedom of the smoothing spline by dropping each data point in turn, and then evaluating how well the resultant spline estimates the missing data point. The data perturbation was repeated 1000 times for each run, and from these simulations, the 99, 95 and 67 % uncertainty intervals were calculated for both the combined far-field relative sea-level record and the first derivative of it (C_{FRS} and D_{FRS} , respectively). These were calculated by ordering the simulations at each time point and taking the corresponding quartiles from the empirical distribution. In Supplementary Materials 2 and 3, we provide histograms that show probability distributions from our runs for four time slices (5, 10, 15 and 20 ka BP), and a plot of examples of individual simulations for our C_{FRS} ensemble run, respectively.

Because we use only far-field sites in our compilation of data (Figure 1), we consider that our probability limits represent a close approximation of the global eustatic sea level history. Although Milne and Mitrovica (2008) required 15-20 m of uncertainty in their model to correct for the isostatic effect within these far-field sea-level records, it is likely that isostatic uncertainties would increase the ‘noise’ in our Monte Carlo analysis, and not produce any artefacts or ‘jumps’ in any individual sea-level records. This we assess by systematically removing individual datasets and then comparing each record with the remaining composite curve. We deliberately do not produce a ‘best’ estimate of that history, because such a ‘line’ reconstruction would have limited validity given the methodological and chronological uncertainties that are present in each data-point. Instead, probability limits are much more robust with respect to the data quality.

3. Results and Discussion

Results from the full dataset simulation for the time period of the LGM to the present-day are presented in Figure 3. Figure 3a shows the concomitant climate history based on the layer-counted GRIP ice core. Figure 3b shows our sea-level reconstruction (C_{FRS}) through time and Figure 3c shows the first time-derivative of the sea-level reconstruction (i.e., the rate of sea-level change) (D_{FRS}). Our findings suggest that the rate of sea-level rise started to accelerate from around 17 ka BP (Figure 3b, c), and that the rates of rise probably exceeded 1m/century between ~15 ka BP and ~8 ka BP. Despite the fact that in Figure 3b the sea-level rise over this time interval appears to have been almost constant, the actual rates of change in Figure 3c indicate two discrete peaks, although these are lower than suggested rates of around 430 cm/century from Barbados alone (Fairbanks, 1989; Stanford et al., 2006).

The first interval of highest rates of sea-level rise began at around the Bølling warming (14.6 ka BP), and lasted until about 12.8 ka BP. Highest rates of rise occurred at ~13.8 ka BP with values of up to 260 cm/century (99 % confidence). Note that the onset of this increase in the rate of deglacial sea-level rise, within the ‘probable’ 67 % probability bracket, does not show as a distinct acceleration but rather as a continuous increase of rates since the onset of the deglaciation (Figure 3c), with rates between 100-130 cm/century. The second interval of highest rates of sea-level rise begins at around 11.5 ka BP and peaks at 10.9 ka BP and 9.5 ka BP (99 % confidence) with values of around 190 cm/century and 250 cm/century, respectively (Figure 3c). However, the 67 % confidence (probable) during this interval only identifies the one peak at 9.5 ka BP with rates of sea-level rise between 130 and 150

cm/century. Thereafter, the rate of sea-level rise gradually drops to near zero at around 6 ka BP, at which time ice-sheets had become similar to the present-day.

Although the coral species *A. palmata* typically lives within the uppermost 5-6 m water-depth (Lighty et al., 1982; Toscano and Macintyre, 2003; Peltier and Fairbanks, 2006), they can exhibit growth rates of up to 14 mm yr⁻¹ and in isolated cases survive in <15 m water depth (Bruckner, 2002). Therefore, we test the sensitivity of our reconstruction to an increase in the depth uncertainty for the fossil corals up to 15 m (i.e., the likely maximum prior to drowning) (Figure 4). There is a very close similarity to our initial 6 m uncertainty ensemble run (Figure 3), although the confidence intervals are slightly increased and the 99 % confidence is more noisy. This indicates that our overall results are robust relative to realistic uncertainty in the coral depth habitat.

Next, we systematically remove individual component datasets from our Monte Carlo simulation and we subtract these results from our full ensemble run (C_{FRS} - see Table 2 for the treatment of each ensemble run). This will illustrate any disproportionate dependence of the overall results on individual component datasets. We then compare each run with the component data that had been removed from it (Figure 5, panels A-E). It is clear that these sub-sampled datasets yield results that are similar to our main reconstruction and typically fall within about ± 3 to 4 m. The largest difference is -5 m (17-14.4 ka BP), which is observed when the Sunda Shelf dataset is removed (Figure 5B). However, as the sea-level curve is primarily constrained by the Sunda Shelf data during this interval, this result is not surprising, and accordingly, our reconstructed probability intervals are significantly widened. When focussing upon the rate of sea-

level change, the removal of the Sunda Shelf dataset does not appreciably change the timing of mwp-1a. Conversely, removal of the Barbados data alters the nature of mwp-1a significantly (Figure 5A). That experiment shows a probable (67 % confidence) increase in the rate of sea-level rise from 17 ka BP, with near constant sea-level rise rates across the Bølling warming. This was followed by an increase in the rate of rise from around 14.2 ka BP, to maximum rates at ~13.4 ka BP, much later than the suggested mwp-1a dating from either Sunda Shelf or Barbados alone (Fairbanks, 1989; Bard et al., 1990a, b; Hanebuth et al., 2000; Fairbanks et al., 2005; Peltier and Fairbanks, 2006).

With respect to the fossil coral records, the maximum difference is observed when removing the Tahiti dataset (Figure 5D). Even so, this difference remains less than 5 m, and thus falls within the 6 m coral depth uncertainty. Figure 6 portrays the same run (C_{FRS-Ta} ; Table 2) as Figure 5D but zooms in on the interval that encompasses mwp-1b (Figure 6). The omitted Tahiti data predominantly plot within the 99 % confidence limits for C_{FRS-Ta} which includes all other data except for Tahiti. This strongly supports recent suggestions that mwp-1b may not have been as large and as sharp as was previously thought (Bard et al., 2010). Our analyses reveal that the global data for far-field sites support a significant post Younger Dryas sea-level rise, but that this occurred in a broad multi-millennial peak in the rates of sea-level rise.

3.1. Mwp-1a

We now focus on the sea-level change at the timing of mwp-1a. Figure 7 identifies sea-level points that sit clearly outside the 99 % confidence envelope in the main

reconstruction (all data, C_{FRS}). These outlier points are numbered HP1, S1-S4 and B1-6 in Figure 7b. We investigate why these data points fall out of the probability envelope, by scrutinising the Huon Peninsula (HP1), Barbados (B1-B6) and Sunda Shelf (S2-S5) sea-level records in more detail for this time interval.

For the Huon Peninsula, one lone fossil coral sample at 79 m water depth, with a U/Th age of 14.61 ± 0.05 ka BP, has been used to identify the earliest possible indication of mwp-1a (HP1 in Figure 7b; Cutler et al., 2003). However, this sea-level indicator clearly lies well above our 99 % confidence interval. Given that this dating was not tested for diagenesis (Cutler et al., 2003), and sits alone and outside of any stratigraphic context, we question this sea-level indicator as a robust marker for mwp-1a.

In the Barbados fossil coral record, sea-level points B1-B6 (Figure 7b) represent the recently added high-precision pre-mwp-1a U/Th datings, which were used to validate the post-14.2 ka BP age for mwp-1a (Fairbanks et al., 2005; Peltier and Fairbanks, 2006; Stanford et al., 2006). However, all of these six points fall below our 99 % confidence interval (Figure 7b). This suggests that these Barbados corals may be underestimating the sea-level depths at this time, although their ‘typical’ 6 m depth uncertainties for *A. palmata* just overlap our reconstructed 99 % confidence interval. These corals may have been growing anomalously deep, possibly in a struggle to keep up with early mwp-1a.

Finally, we consider the Sunda Shelf sea-level record, and we first outline a set of criteria by which to assess the data. The red symbols in Figure 2c, and asterisked

symbols in Figure 7b highlight results from *in situ* mangrove roots on Sunda Shelf (Hanebuth et al., 2000). These are considered more reliable than the other results (black), which were described as loose wood fragments and macro-fibres, which are more likely to have undergone reworking (Hanebuth et al., 2000). Because of this reworking potential, we consider (after the *in situ* roots) the youngest ages from the wood fragments/macro-fibres to be the most accurate. Error may also result from compaction due to dewatering and coring, contamination by younger material and by the displacement of vegetation from higher elevations during spring tides (Toscano and Macintyre, 2003).

Figure 7b shows that between ~15 and ~14.2 ka BP, the re-calibrated sea-level points from the Sunda Shelf plot closely around (or just above) the six new U/Th dated sea-level points from Barbados (B1-B6) (Fairbanks et al., 2005; Peltier and Fairbanks, 2006). Using the above criteria, this horizon of sea-level indicators is validated by a dating on *in situ* mangrove root fibres, which has an age range of 14.121-14.969 ka BP (2σ) that overlaps well with our 67 % probability interval. Further validation is given by two datings on separate pieces of mangrove wood taken from the same depth in core 18301-2, which yielded dates 14.123-15.025 ka BP (2σ) and 14.021-14.890 ka BP (2σ). We note that although the mean age for these sea-level points sit just outside the 95 % confidence interval (Figure 7b), indicating possible displacement by compaction, their 2σ uncertainties overlap the 99 % probability curve. Given the reproducibility of the ^{14}C age, the reworking potential of loose wood fragments, and the close agreement with the Barbados sea-level data (Figures 3 and 7b), we consider these ^{14}C age values as robust validation for the most reliable age of the *in situ* mangrove wood at 14.121-14.969 ka BP (2σ).

In situ mangrove root fibres (S1 in Figure 7b) that were dated at 13.96 ka BP, with a relatively ‘tight’ 2σ range of 13.781-14.138 ka BP, give the first clear indication of the mwp-1a sea-level rise at Sunda Shelf. Two further datings validate this sea-level indicator, one obtained from macro-fibres and the other a loose piece of wood. These have slightly older ages of 13.858-14.538 ka BP (2σ) and 14.021-14.890 ka BP (2σ), respectively. These observations, which are fully enclosed within our 99 % probability interval (Figure 7b), plot well within the 95 % probability interval of our reconstruction based on removal of the Sunda Shelf data (Figure 5B), which indicates that the inferred increase in the rate of sea-level rise at ~ 14 ka BP is valid.

Four Sunda Shelf data points (S2–S5 in Figure 7b) clearly plot above the 99 % confidence interval of our modelled sea-level curve, one of which is a dating on *in situ* mangrove root material; the best constrained depth indicator from the Sunda Shelf. However, these are the only data from marine sediment cores 18309-2 and 18308-2 (*Supplementary Information* with Hanebuth et al., 2000), and we therefore consider that these dating may be stratigraphically out of place in relation to the series of coherent datings from cores 18301-2 (the same site as core 18300-2), which includes the oldest date for mwp-1a on the *in situ* mangrove root (14.121-14.969 ka BP (2σ)).

Despite the fact that the Barbados corals may be under-estimating the reconstructed early sea-level rise between 14.5 and 14.1 ka BP, it is clear from our reconstruction that the peak freshwater discharge event of mwp-1a occurred somewhat later, at around 13.8 ka BP (Figure 7c). Core logs for Sunda Shelf (*Supplementary*

Information with Hanebuth et al., 2000) show significant depositional hiatuses in most cores after about 14 ka BP (i.e., when the pre-mwp-1a lowstand mangrove forests drowned). A dating of around 13.3 ka BP in core 18322, taken after the transition from ‘high glacial soils’ to ‘shoreline’ deposits (*Supplementary Information* with Hanebuth et al., 2000), represents the oldest Sunda Shelf evidence of a high post-mwp-1a sea-level. Based on our 99 % confidence margins, the peak rate of sea-level rise during mwp-1a was 260 cm/century (Figure 7c), and we propose that the mangrove forests/coastal swamps may not have been able to accrete fast enough to keep up with this rapid sea-level rise. Therefore, we suggest that the peak sea-level rise of mwp-1a may be represented on Sunda Shelf by a depositional hiatus, bracketed by the aforementioned datings of 13.8 ka BP and 13.4 ka BP, using the minimum 2σ age uncertainties (Figure 5b). We also consider that the large depositional hiatus in the Barbados record after sample RGF 9-8-2 (14.082 ka BP) represents the main sea-level jump of mwp-1a, when the coral reef could no longer accrete at a fast enough rate to keep up with the sea-level rise, and drowned.

It is clear from our C_{FRS} reconstruction, using the 67 % confidence limits, that the timing of the onset of mwp-1a cannot really be distinguished from the timing of Bølling warming, although a slight acceleration is observed at around 14.4 ka BP, post dating the sharp warming event (Figure 7c). Our results also highlight data points that clearly lie outside the 99 % confidence interval. These appear to be compromised, but it remains to be established whether this is due to age uncertainties, depth uncertainties, or site-specific isostatic issues. Our work furthermore identifies where either additional data are required and/or better constraints on uncertainties are needed to better resolve timing discrepancies between sea-level records (e.g., during the early

deglaciation and across the Bølling warming). We look forward to including the latest drilling results from Tahiti once these become available (Bard et al., *unpublished*).

Conclusions

Using previously published sea-level records from Barbados, the Sunda Shelf, Tahiti, Huon Peninsula, Bonaparte Gulf and the Caribbean Sea, a Monte Carlo experiment was used to assess the uncertainties in these far-field datasets of relative sea-level change, and we assume that the calculated 67 % probability interval closely approximates the global eustatic change. Overall, our results show that from around 17 ka BP sea-level rise started to accelerate into the deglaciation. Two robust maxima in the rate of sea-level rise have been identified (mwp-1a and mwp-1b). Mwp-1a is of a multi-centennial to millennial nature, and started at around the timing of the Bølling warming (14.6 ka BP). Its character is not so much that of the sharp spike described before (Fairbanks, 1989; Stanford et al., 2006), but more like a broader culmination of the continuous increase in the rates of rise that started at around 17 ka BP. Mwp-1b is expressed as a broad multi-millennial peak, which started to build up just after the end of the Younger Dryas (11.3 ka BP). Both maxima were found to be robust with respect to systematic removal of individual component datasets from our statistical analyses.

Results from our Monte Carlo experiment imply an age for the maximum of mwp-1a at 13.8 ka BP, which post-dated the Bølling warming. Careful scrutiny and re-evaluation of both the Sunda Shelf and Barbados sea-level records now reconciles the deglacial sea-level history between these two datasets, and between these and the

other data sets for the last deglaciation. These results confirm previous suggestions that either the ocean-climate system behaves non-linearly to freshwater forcing, or that the location and/or depth distribution of meltwater input into the ocean was more important than the magnitude or rate of that input (e.g., Stanford et al., 2006; Obbink et al., 2010; Thornally et al., 2010).

Acknowledgements

We would like to thank Dr. A. Thomas and the two anonymous reviewers of this manuscript for their insightful and constructive suggestions and comments. This study contributes to Natural Environment Research Council projects NE/H004424/1 and NE/D001773/1. We would also like to thank Mrs K. Davis, as well as Dr. M. Siddall for his constructive feedback. The compiled data (as input into the Monte Carlo analysis), can be found along with the R script and the output data (the 67, 95 and 99 % probability ranges for our C_{FRS} reconstruction) on the British Oceanographic Data Centre (BODC) website, and at www.soes.soton.ac.uk/staff/ejr/ejrhome

References

- Andersen, K. K., Svensson, A., Johnsen, S. J., Rasmussen, S. O., Bigler, M., Röthlisberger, R., Ruth, U., Siggaard-Andersen, M.-L., Steffensen, J. P., Dahl-Jensen, D., Vinther, B. M., Clausen, H. B., 2006. The Greenland Ice Core Chronology 2005, 15–42 ka. Part 1: constructing the time scale. *Quaternary Science Reviews* 25, 3246–3257.
- Austin, W. E. N., Kroon, D., 2001. Deep sea ventilation of the northeastern Atlantic during the last 15,000 years. *Global and Planetary Change* 30, 13-31.
- Bard, E., Hamelin, B., Fairbanks, R. G., Zindler, A., 1990a. Calibration of the ^{14}C timescale over the past 30,000 years using mass spectrometric U-Th ages from Barbados corals. *Nature* 345, 405-410.
- Bard, E., Hamelin, B., Fairbanks, R. G., 1990b. U/Th ages obtained by mass spectrometry in corals from Barbados – sea-level during the past 130,000 years. *Nature* 346, 456-458.
- Bard, E., Hamelin, B., Arnold, M., Montaggioni, L., Cabioch, G., Faure, G., Rougerie, F., 1996. Sea level record from Tahiti corals and the timing of deglacial meltwater discharge. *Nature* 382, 241-244.
- Bard, E., Hamelin, B., Delanghe-Sabatier, D., 2010. Deglacial Meltwater Pulse 1B and Younger Dryas sea levels revisited with boreholes at Tahiti. *Science* 327, 1235-1237.
- Basset, S. E., Milne, G. A., Mitrovica, J. X., Clark, P.U. 2005. Ice sheet and solid earth influences on far-field sea-level histories. *Science* 309, 925-928.
- Bruckner, A.W., 2002. Proceedings of the Caribbean *Acropora* Workshop: Potential

- Application of the U.S. Endangered Species Act as a Conservation Strategy.
NOAA Technical Memorandum NMFS-OPR-24, Silver Spring, MD pp 101.
- Chappell, J., Polach, H. 1991. Post-glacial sea-level rise from a coral record at Huon Peninsula, Papua New Guinea. *Nature* 147-149.
- Clark, P. U., Mitrovica, J. X., Milne, G. A., Tamisiea, M. E., 2002. Sea-level fingerprinting as a direct test for the source of global meltwater pulse 1a. *Science* 295, 2438-2441.
- Clark, P.U., Dyke, A. S., Shakun, J. D., Carlson, A. E., Clark, J., Wohlfarth, B., Mitrovica, J. X., Hostetler, S. W., McCabe, A. M. 2009. The Last Glacial Maximum. *Science* 325, 710-714.
- Cutler, K. B., Edwards, R. L., Taylor, F. W., Cheng, H., Adkins, J., Gallup, C. D., Cutler, P. M., Burr, G. S., Bloom, A. L., 2003. Rapid sea-level fall and deep-ocean temperature change since the last interglacial Period. *Earth and Planetary Science Letters* 206, 253–271.
- Digerfeldt, G., Hendry, M. D. 1987. An 8000 yr Holocene sea-level records from Jamaica: implications for interruption of Caribbean reef and coastal history. *Coral Reefs* 5, 165-169.
- Fairbanks, R. G., 1989. A 17,000-year glacio-eustatic sea level record: Influence of glacial melting rates on the Younger Dryas event and deep-ocean circulation. *Nature* 342, 637-642.
- Fairbanks, R. G., Mortlock, R. A., Chiu, T.-C., Cao, L., Kaplan, A., Guilderson, T. P., Fairbanks, T. W., Bloom, A. L., Grootes, P. M., Nadeau, M.-J., 2005. Radiocarbon calibration curve spanning 0 to 50,000 years BP based on paired $^{230}\text{Th}/^{234}\text{U}/^{238}\text{U}$ and ^{14}C dates on pristine corals. *Quaternary Science Reviews*

24, 1781-1796.

Green, P. J., Silverman, B. W., 1994 *Nonparametric Regression and Generalized Linear Models: A Roughness Penalty Approach*. Chapman and Hall.

Hanebuth, T., Stattegger, K., Grootes P. M., 2000. Rapid flooding of the Sunda shelf: A late-glacial sea-level record. *Science* 288, 1033-1035.

Hanebuth, T., Stattegger, K., Bojanowski, A. 2009. Termination of the Last Glacial Maximum sea-level lowstand: The Sunda Shelf data revisited. *Global and Planetary Change*, 66, 76-84.

Lambeck, K., Yokoyama, Y., Purcell, T., 2002. Into and out of the Last Glacial Maximum: Sea level change during Marine Oxygen Isotope Stages 3 and 2. *Quaternary Science Reviews* 21, 343-360.

Lighty, R.G., Macintyre, I. G., Stuckenrath, R., 1982. *Acropora palmata* reef framework: a reliable indicator of sea-level in the western Atlantic for the past 10,000 years. *Coral Reefs* 1, 125–130.

Liu, J. P., Milliman, J., 2004. Reconsidering Melt-water Pulses 1A and 1B: Global Impacts of Rapid Sea-level rise. *Journal of Ocean University of China* 3, 183-190.

Kroon, D., Austin, W. E. N., Chapman, M. R., Ganssen, G. M., 1997. Deglacial surface circulation changes in the northeastern Atlantic: Temperature and salinity records off NW Scotland on a century scale. *Paleoceanography* 12, 755-763.

Macintyre I.G., Multer H.G., Zankl H.L., Hubbard D.K., Weiss M.P., Stuckenrath R. (1985) Growth and depositional facies of a windward reef complex (Nonsuch Bay, Antigua, W.I.) *Proc 5th Int Coral Reef Congr Tahiti* 6, 605–610

Macintyre, I. G., Littler, M. M., Littler, D. S. 1995. Holocene history of Tobacco

- Range, Belize, Central America, Atoll Res Bull 430, 1-18.
- Macintyre I.G., Toscano M.A., Lighty R.G., Bond G.B. (2004) Holocene history of the mangrove islands of Twin Cays, Belize, Central America. Atoll Res Bull 510, 1-16.
- McManus, J. F., Francois, R., Gherardi, J.-M., Keigwin, L. D. & Brown-Leger, S., 2004. Collapse and rapid resumption of Atlantic meridional circulation linked to deglacial climate changes. Nature 428, 834-837.
- Milne, G. A., and Mitrovica, J. X. 2008. Searching for eustasy in deglacial sea-level histories, Quaternary Science Reviews, 27, 2292-2302.
- Obbink, E. A., Carlson, A. E., Klinkhammer, G. P. 2010. Eastern North American freshwater discharge during the Bølling-Allerød warm periods. Geology 38, 171-174.
- Peltier, W. R., Fairbanks, R. G., 2006. Global ice volume and Last Glacial Maximum duration from an extended Barbados sea-level record. Quaternary Science Reviews 25, 3322-3337.
- R Development Core Team, 2010. R: A language and environment for statistical computing. R Foundation for Statistical Computing, Vienna, Austria. ISBN 3-900051-07-0, URL <http://www.R-project.org>.
- Rasmussen, S .O., Andersen, K. K., Svensson, A. M., Steffensen, J. P., Vinther, B. M., Clausen, H. B., Siggaard-Andersen, M.-L., Johnsen, S. J., Larsen, L. B., Dahl-Jensen, D., Bigler, M., Röthlisberger, R., Fischer, H., Goto-Azuma, K., Hansson, M. E., Ruth U., 2006. A new Greenland ice core chronology for the last glacial termination. Journal of Geophysical Research 111, D06102, doi:10.1029/2005JD006079.
- Rasmussen, S.O., Seierstad, I. K., Andersen, K. K., Bigler, M., Dahl-Jensen, D.,

- Johnsen, S. J., 2008. Synchronization of the NGRIP, GRIP, and GISP2 ice cores across MIS 2 and palaeoclimatic implications. *Quaternary Science Reviews* 27, 18-28.
- Reimer, P. J., Baillie, M. G. L., Bard, E., Bayliss, A., Beck, J. W., Bertrand, C. J. H., Blackwell, P. G., Buck, C. E., Burr, G. S., Cutler, K. B., Damon, P. E., Edwards, R. L., Fairbanks, R. G., Friedrich, M., Guilderson, T. P., Hogg, A. G., Hughen, K. A., Kromer, B., McCormac, G., Manning, S., Ramsey, C. B., Reimer, W. R., Remmele, S., Southon, J. R., Stuiver, M., Talamo, S., Taylor, F. W., van de Plicht, J., Weyhenmeyer, C. E., 2004. IntCal04 terrestrial radiocarbon age calibration, 0-26 cal kyr BP. *Radiocarbon* 46, 1029-1058.
- Reimer, P. J., Baille, M. G. L., Bard, E., Bayliss, A., Beck, J. W., Blackwell, P. G., Bronk Ramsey, C., Buck, C. E., Burr, G. S., Edwards, R. L., Friedrich, M., Grootes, P. M., Guilderson, T. P., Hajdas, I., Heaton, T. J., Hogg, A. G., Hughen, K. A., Kaiser, K. F., Kromer, B., McCormac, G., Manning, S. W., Reimer, R. W., Richards, D. A., Southon, J. R., Talamo, S., Turney, C. S. M., van der Plicht, J., Weyhenmeyer, C. E. 2009. INTCAL09 and MARINE09 radiocarbon age calibration curves, 0-50,000 yrs Cal BP. *Radiocarbon*, 51, 1111-1150.
- Robbin, D. M. (1984) A new Holocene sea-level curve for the upper Florida Keys and Florida reef tract. In: Gleason, P. J. (Ed) *Environments of South Florida, present and past*. Miami Geological Society, pp.437-458.
- Severinghaus, J.P., Brook E. J., 1999. Abrupt climate change at the end of the last glacial period inferred from trapped air in polar ice. *Science* 286, 930-934.
- Shinn, E. A., Hudson, J. H., Halley, R. B., Lidz, B., Robbin, D. M., Macintyre, I. G. (1982) Geology and sediment accumulation rates at Carrie Bow Cay, Belize,

- Smithsonian Contr. Mar. Sci., 12, 63-75.
- Siddall, M., Rohling, E. J., Almogi-Labin, A., Hemleben, C., Meischner, D., Schmelzer, I., Smeed, D. A., 2003. Sea-level fluctuations during the last glacial cycle. *Nature*, 423, 853-858.
- Stanford, J. D., Rohling, E. J., Hunter, S. E., Roberts, A. P., Rasmussen, S. O., Bard, E., McManus, J., Fairbanks R. G., 2006. Timing of meltwater pulse 1a and climate responses to meltwater injections. *Paleoceanography* 21, 4, PA4103. (doi:10.1029/2006PA001340).
- Svensson, A., Andersen, K. K., Bigler, M., Clausen, H. B., Dahl-Jensen, D., Davies, S. M., Johnsen, S. J., Muscheler, R., Rasmussen, S. O., Röthlisberger, R., Steffensen, J. P., Vinther, B. M., 2006. The Greenland Ice Core Chronology 2005, 15-42 ka. Part 2: Comparison to other records. *Quaternary Science Reviews* 25, 23-24.
- Thornalley, D. J. R., McCave, I. N., Elderfield, H. 2010. Freshwater input and abrupt deglacial climate change in the North Atlantic. *Paleoceanography* 25, PA1201, doi: 10.1029/2009PA001772.
- Toscano, M. A., Lundberg, J. (2003) Early Holocene sea-level record from submerged fossil reefs on the southeast Florida margin. *Geology*, 25, 255-258.
- Toscano, M. A., Macintyre, I. G., 2003. Corrected western Atlantic sea-level curve for the last 11,000 years based on calibrated ¹⁴C dates from *Acropora palmate* framework and intertidal mangrove peat. *Coral Reefs* 22, 257-270.
- Weaver, A.J., Saenko, O. A., Clark, P. U., Mitrovica, J. X., 2003. Meltwater pulse 1A from Antarctica as a trigger of the Bølling-Allerød warm interval. *Science* 299, 1709-1713.
- Yokoyama, Y., Lambeck, K., Deckker, P. D., Johnston, P., Fifield, L. K., 2000.

Timing of Last Glacial Maximum from observed sea level minima. *Nature* 406, 713-716.

Yokoyama, Y., Deckker, P. D., Lambeck, K., Johnston, P., Fifield, L. K. 2001. Sea-level at the Last Glacial Maximum: evidence from northwestern Australia to constrain ice volumes for oxygen isotope stage 2. *Paleoceanography, Paleoclimatology, Paleoecology* 165, 281-297.

Tables

Table 1. Data sources for our Monte Carlo experiment

Location	Dating Method	Material	Tectonic correction	Source reference
Barbados	U/Th	Fossil corals	-0.34 m/kyr	Fairbanks (1989), Bard et al. (1990a,b) Peltier & Fairbanks (2006)
Sunda Shelf	AMS ¹⁴ C	Mangrove wood fragments, wood and marine carbonate	-	Hanebuth et al. (2000; 2009)
Bonaparte Gulf	AMS ¹⁴ C	Marine carbonate	-	Yokoyama et al. (2000; 2001)
Tahiti	AMS ¹⁴ C and U/Th	Fossil coral	0.25 m/kyr	Bard et al. (1996; 1998; 2010)
Huon Peninsula	AMS ¹⁴ C and U/Th	Fossil coral	-1.9 m/kyr, 2.6 m/kyr, 2.1 m/kyr	Chappell & Polach (1991), Cutler et al. (2003)
Florida Keys	AMS ¹⁴ C	Peat samples	-	Macintyre et al. (1995), Shinn et al. (1982), Robbin, (1984), Digerfeldt & Hendry (1987), Toscano & Macintyre (2003)
Panama, Florida Keys, Barbados and the Bahamas	AMS ¹⁴ C	Fossil Coral	-	Lighty et al. (1982) Macintyre et al. (1985), Toscano and Lundberg (1998)

Table 2. Monte Carlo ensemble runs

Ensemble run	Data used
C _{FRS}	Barbados, Sunda Shelf, Bonaparte Gulf, Tahiti, Huon Peninsula and Caribbean Sea/Florida Keys.
C _{FRS-Ba}	Sunda Shelf, Bonaparte Gulf, Tahiti, Huon Peninsula and Caribbean Sea/Florida Keys.
C _{FRS-Su}	Barbados, Bonaparte Gulf, Tahiti, Huon Peninsula and Caribbean Sea/Florida Keys.
C _{FRS-Bo}	Barbados, Sunda Shelf, Tahiti, Huon Peninsula and Caribbean Sea/Florida Keys.
C _{FRS-Ta}	Barbados, Sunda Shelf, Bonaparte Gulf, Huon Peninsula and Caribbean Sea/Florida Keys.
C _{FRS-Hu}	Barbados, Sunda Shelf, Bonaparte Gulf, Tahiti and Caribbean Sea/Florida Keys.

Figures

Figure 1. The predicted total relative sea level (RSL) change minus the model eustatic component for a time window extending from 21 ka BP (A) and 6 ka BP (B) to the present-day. These predictions (departures from the eustatic change) are reproduced from Milne and Mitrovica (2008), who used the Basset et al. (2005) ice model and associated Earth model in their study. The ice and Earth model produced an optimal fit to a number of far-field records. The zero contours show where RSL is equal to the modelled eustatic value. The red and blue colours indicate where sea-level is greater or less than the eustatic value. Ta = Tahiti, Ba = Barbados, Bo = Bonaparte Gulf, Su = Sunda Shelf and Hu = Huon Peninsula. Crosses show the location of datasets used in the Toscano and Macintyre (2003) compilation.

Figure 2a. The GRIP ice core $\delta^{18}\text{O}$ record on the GICC05 timescale on the basis of layer-counting (Andersen et al., 2006; Svensson et al., 2006; Rasmussen et al., 2006; 2008). b. The U/Th-dated *Acropora palmata* corals from Barbados in black, which are corrected for a constant tectonic uplift of 0.34 m kyr^{-1} (Fairbanks et al., 2005; Peltier and Fairbanks, 2006) c. The ^{14}C dated Sunda Shelf sea level record (re-calibrated from Hanebuth et al., 2000). Symbols indicate the mean ages and those that are plotted with only their 2σ error bars represent ages with calibrated multiple 1σ probabilities. Datings on *in situ* roots and root fibres from the Sunda Shelf are shown in red, with their 2σ error bars. The green and blue bars represent the inferred timings of mwp-1a from the Sunda Shelf and Barbados sea-level records, respectively.

Figure 3. Monte Carlo experiment results using a 6m coral depth uncertainty. a. The GRIP ice core $\delta^{18}\text{O}$ record on the GICC05 timescale (Andersen et al., 2006; Svensson et al., 2006; Rasmussen et al., 2006; 2008). b. The modelled sea-level probabilities are shown alongside the data used to construct the Monte Carlo simulations. The error bars shown represent the total uncertainties used in our reconstruction (see supplementary material 1) c. The first derivative of the reconstructed sea-level change. In panels b and c, 100 of the simulations are shown in light grey.

Figure 4. Same as in Figure 3, except a 15 m depth uncertainty for the corals was used.

Figure 5 A-E. Comparison of the Monte Carlo experiment runs after removal of datasets out of the original Monte Carlo experiment (see Table 2). a. The GRIP ice core $\delta^{18}\text{O}$ record on the GICC05 timescale on the basis of layer-counting (Andersen et al., 2006; Svensson et al., 2006; Rasmussen et al., 2006; 2008). b. 67, 95 and 99 % confidence intervals for the modelled sea-level curve, compared to the dataset that was removed from the run c. the difference between the 67, 95 and 99 % probability intervals for the ensemble runs (see Table 2). d. the first derivative of b. e. the difference between d and the original, full Monte Carlo experiment.

Figure 6. Same as Figure 5D, but for 8 to 14 ka BP.

Figure 7. Same as Figure 3, but for the time period 12 to 16 ka BP. The datasets discussed in the main text are highlighted by thicker symbols. Red asterisks denote the mean ages of *in situ* mangrove root samples from the Sunda Shelf. Numbered

samples are those that lie outside the 99 % confidence limits and are discussed in the main text.

Figure 1a

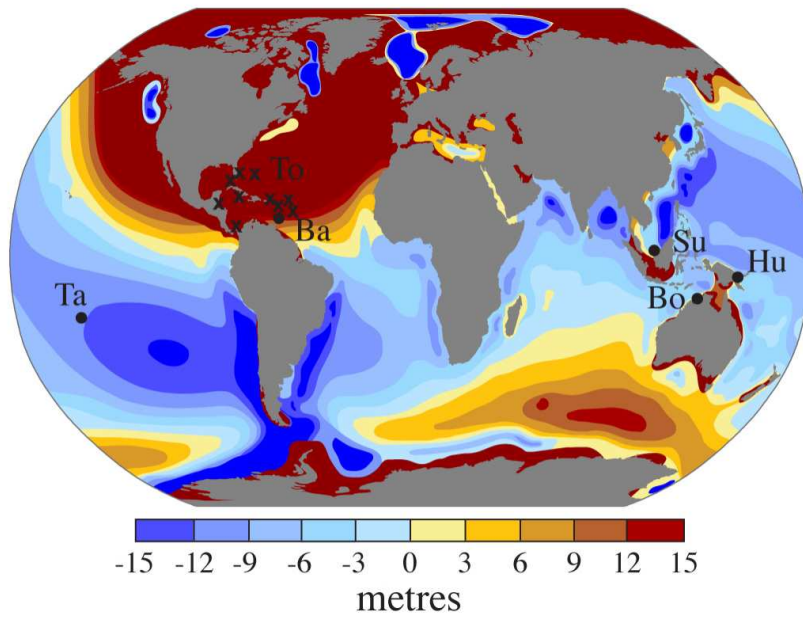


Figure 1b

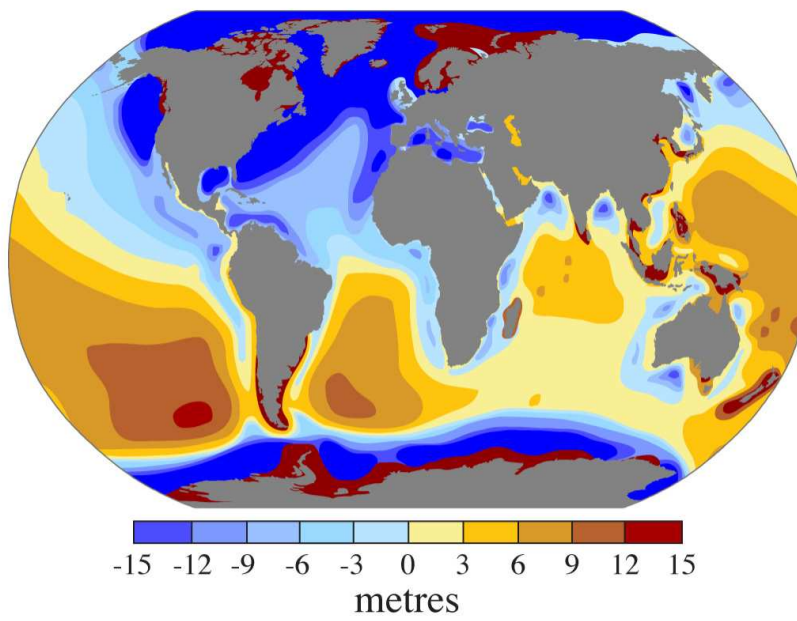


Figure 2

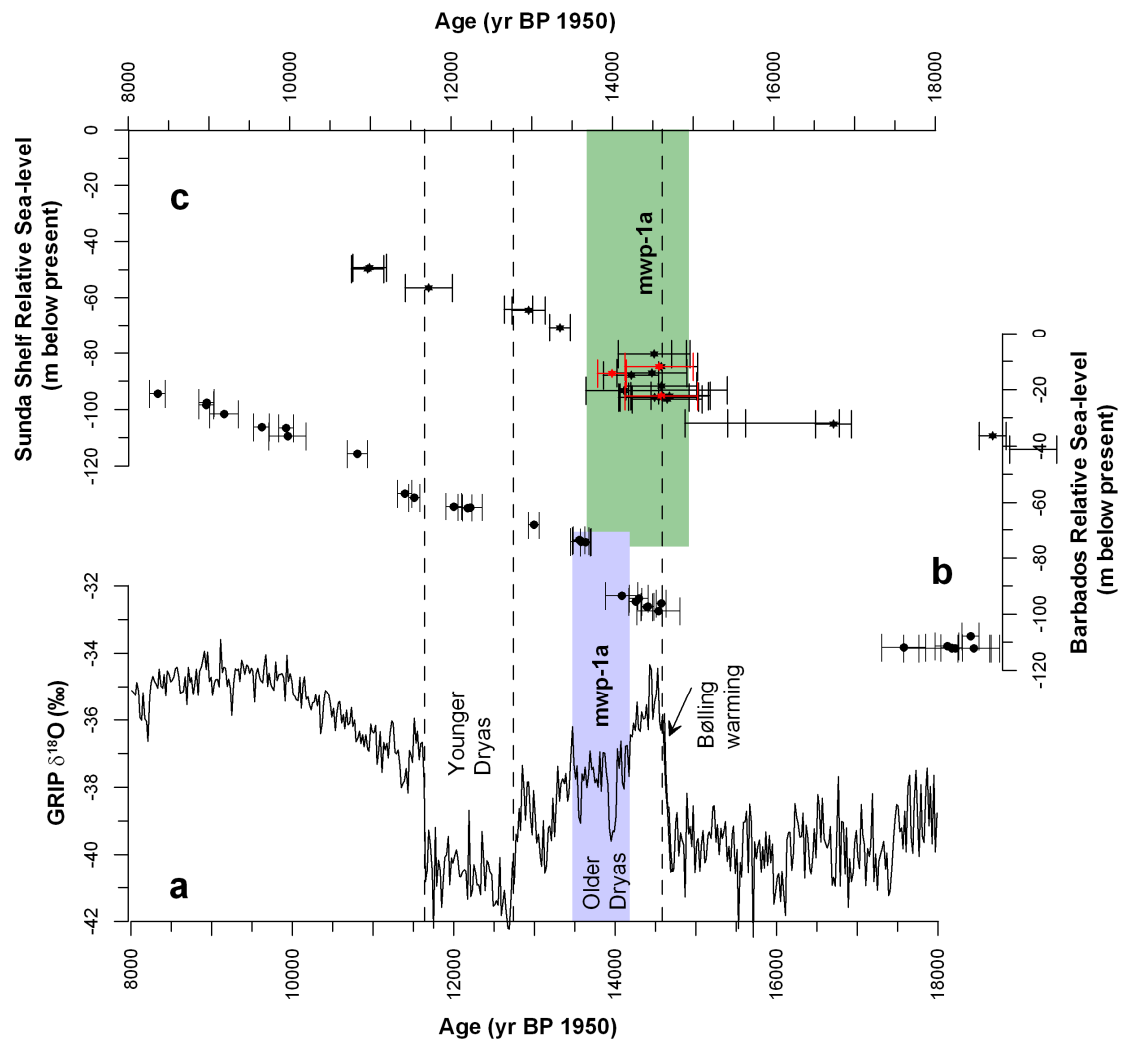


Figure 3

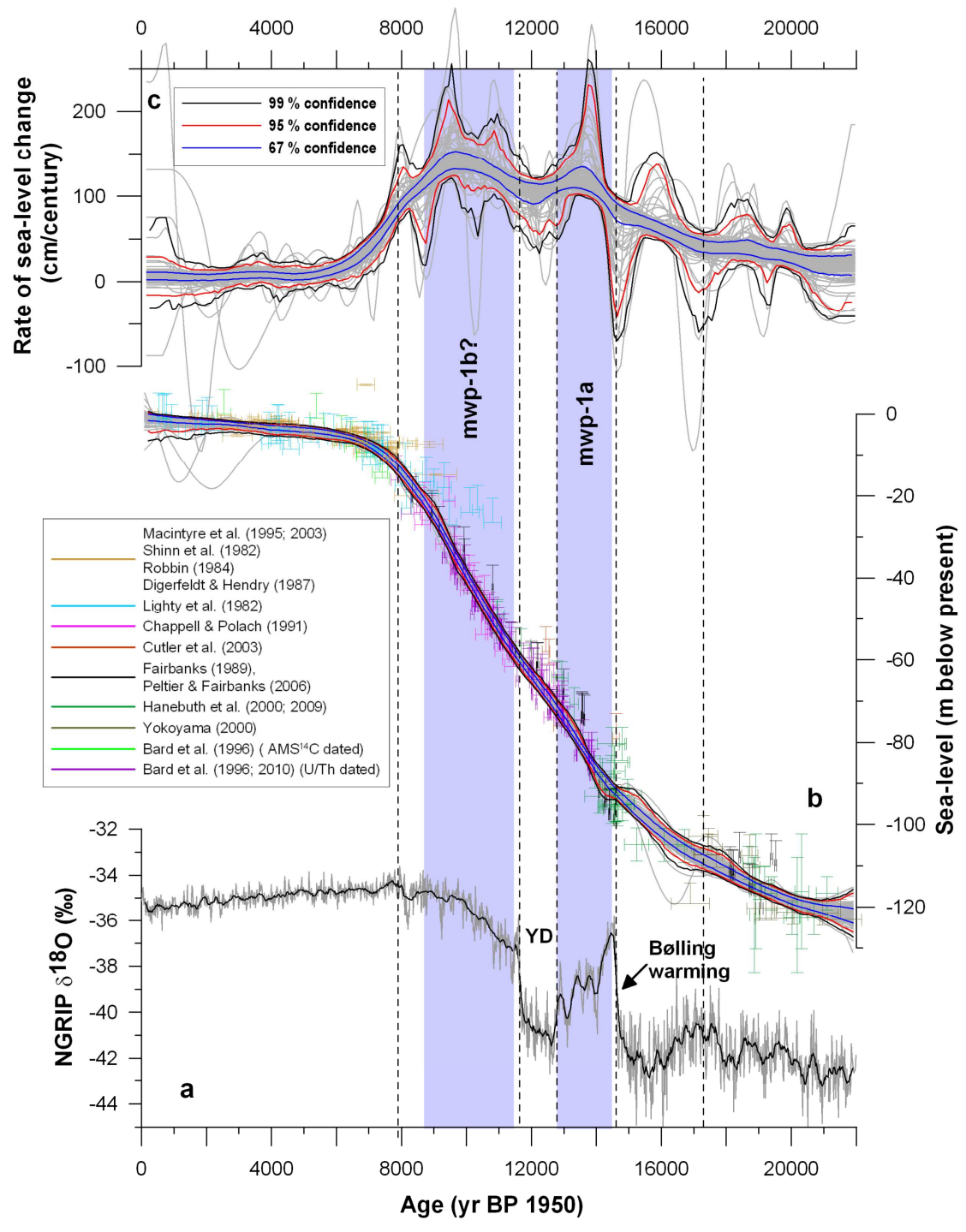


Figure 4

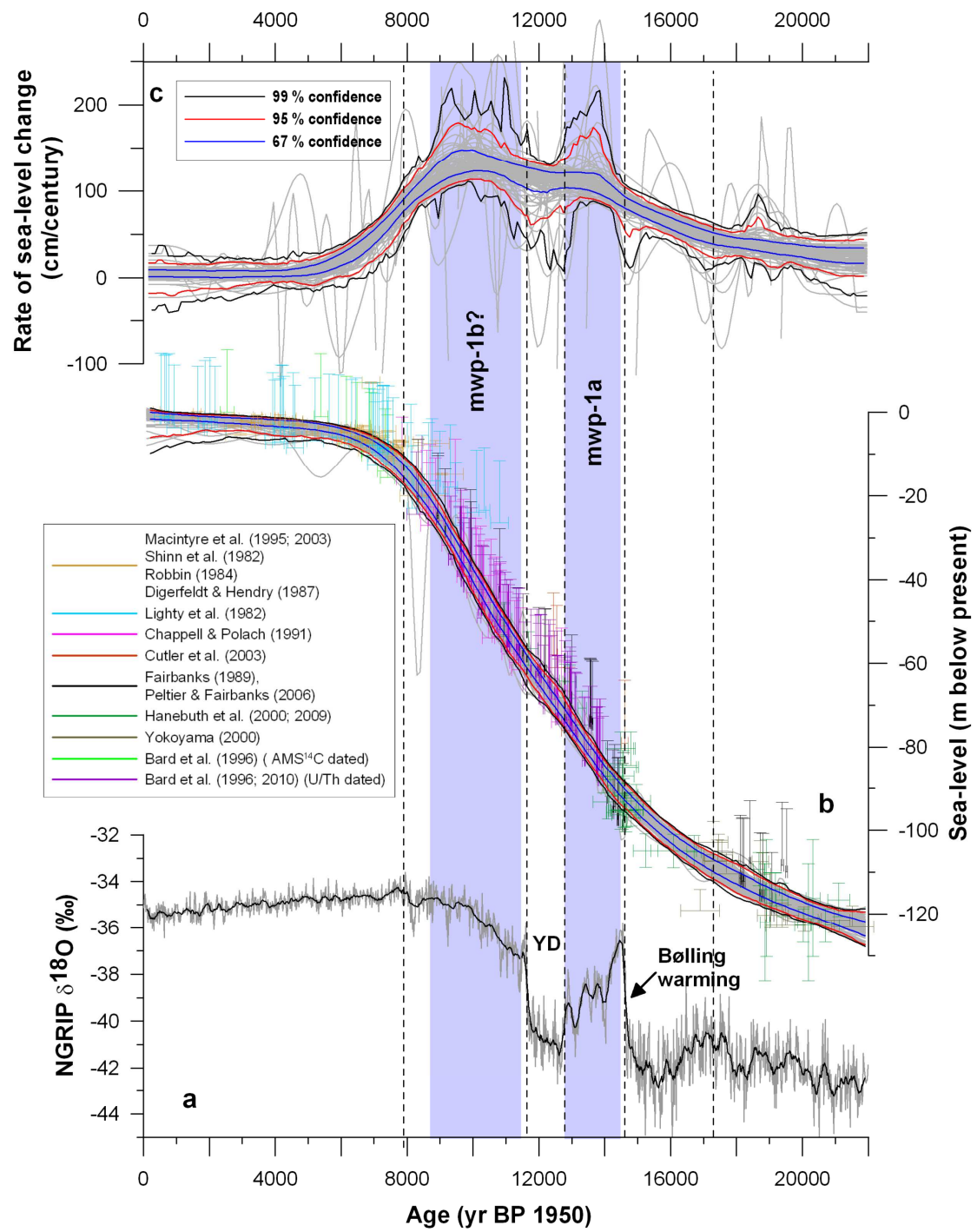


Figure 5

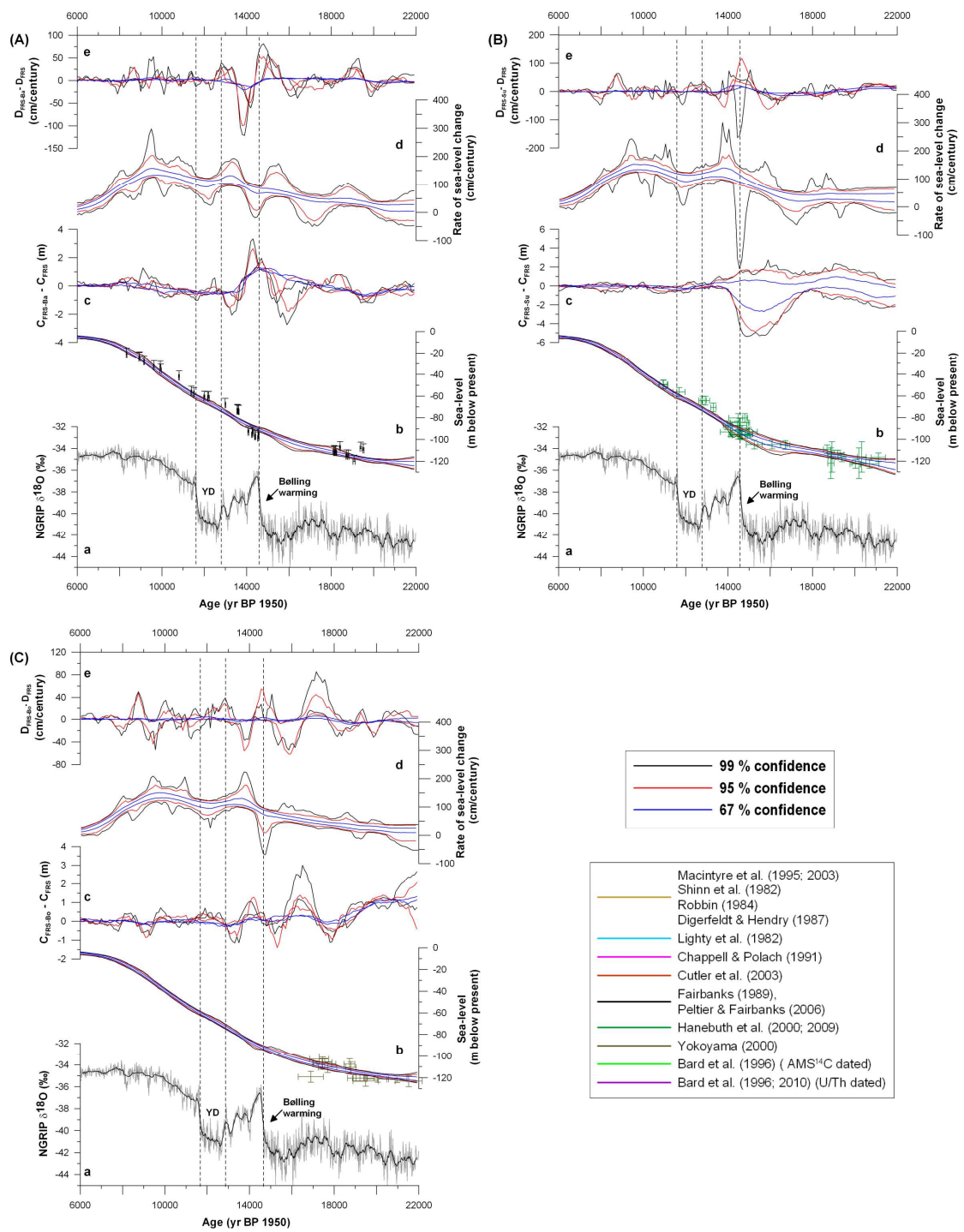


Figure 5 cont.

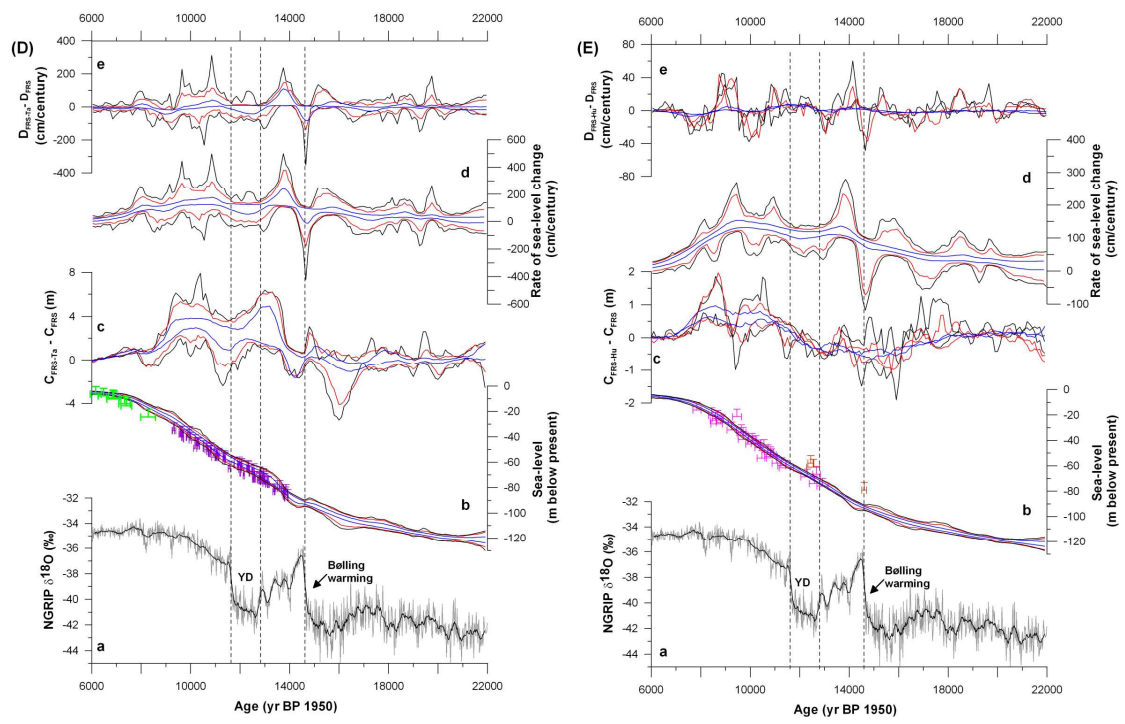


Figure 6

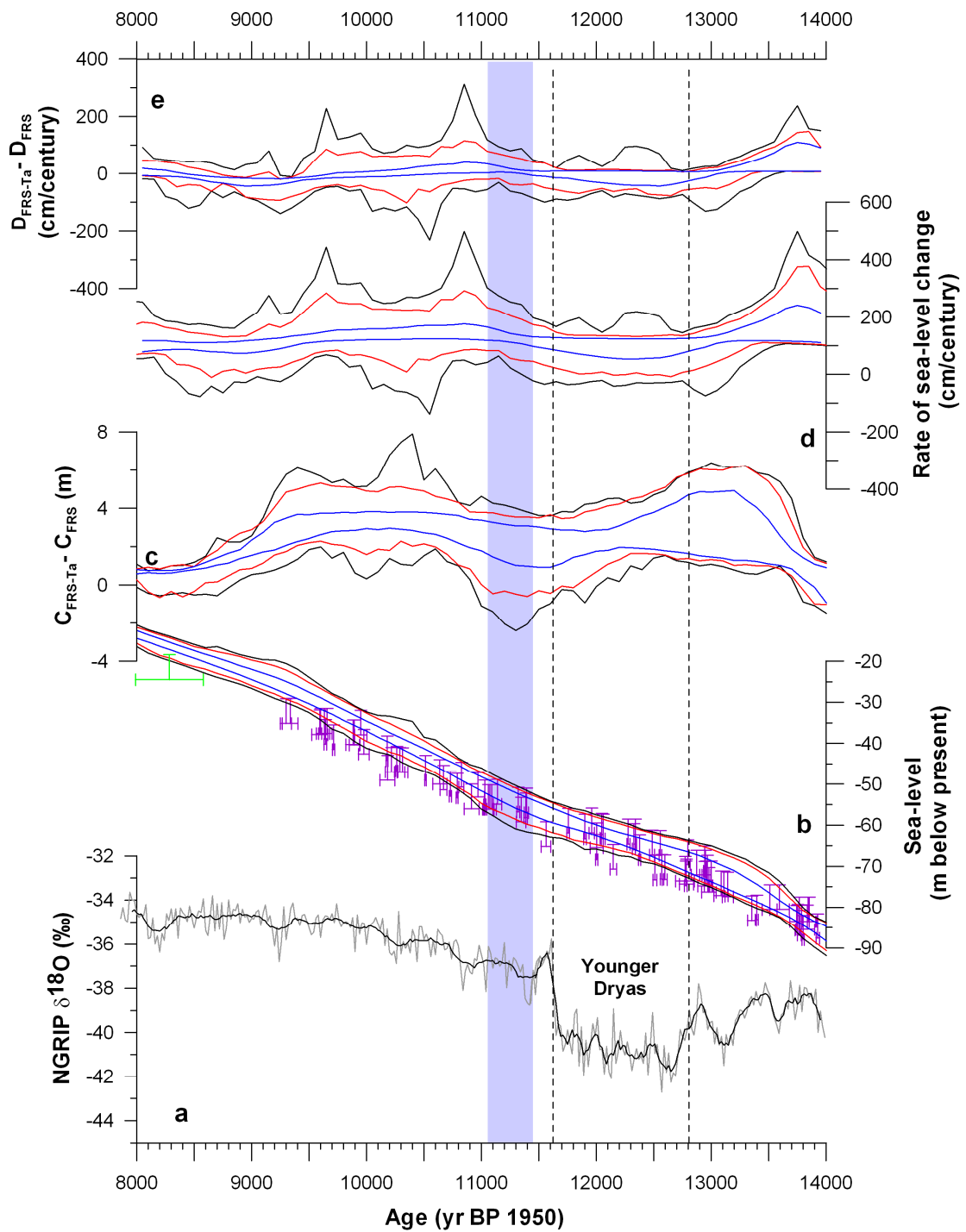


Figure 7

